Accepted Manuscript

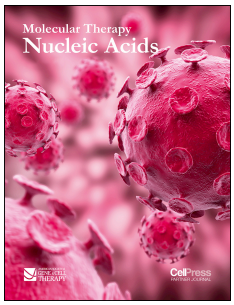

Locked Nucleic Acid gapmers and conjugates induce potent silencing of *ADAM33*, an asthma-associated metalloprotease with nuclear-localized mRNA

Hannah M. Pendergraff, Pranathi Meda Krishnamurthy, Alexandre J. Debacker, Michael P. Moazami, Vivek K. Sharma, Liisa Niitsoo, Yong Yu, Yen Nee Tan, Hans Michael Haitchi, Jonathan K. Watts

PII: S2162-2531(17)30198-1

DOI: 10.1016/j.omtn.2017.06.012

Reference: OMTN 91

To appear in: *Molecular Therapy: Nucleic Acid*

Received Date: 5 March 2017

Revised Date: 15 June 2017

Accepted Date: 16 June 2017

Please cite this article as: Pendergraff HM, Krishnamurthy PM, Debacker AJ, Moazami MP, Sharma VK, Niitsoo L, Yu Y, Tan YN, Haitchi HM, Watts JK, Locked Nucleic Acid gapmers and conjugates induce potent silencing of *ADAM33*, an asthma-associated metalloprotease with nuclear-localized mRNA, *Molecular Therapy: Nucleic Acid* (2017), doi: 10.1016/j.omtn.2017.06.012.

Locked Nucleic Acid gapmers and conjugates induce potent silencing of *ADAM33*, an asthma-associated metalloprotease with nuclear-localized mRNA

Hannah M. Pendergraff[1,2,3], Pranathi Meda Krishnamurthy[4], Alexandre J. Debacker[1,2,4], Michael P. Moazami[1,2,4], Vivek K. Sharma[1,2,4], Liisa Niitsoo[1,2], Yong Yu[5], Yen Nee Tan[5], Hans Michael Haitchi[2,6,7]*, Jonathan K. Watts[1,2,4]*

[1]Department of Chemistry and [2]Institute for Life Sciences, University of Southampton, SO17 1BJ, UK, [3]Current Address: Roche Innovation Center Copenhagen A/S, DK 2970 Hørsholm, Denmark, [4]RNA Therapeutics Institute and Department of Biochemistry and Molecular Pharmacology, UMass Medical School, Worcester, MA, 01605, USA, [5]Institute of Materials Research and Engineering, A*STAR, 138634, Singapore, [6]Clinical and Experimental Sciences, Faculty of Medicine, University of Southampton, SO16 6YD, [7]NIHR Southampton Respiratory Biomedical Research Unit at University Hospital Southampton NHS Foundation Trust, Southampton, SO16 6YD, UK

*Correspondence may be addressed to HMH or JKW. HMH: Tel: +44 (0)23 8120 8410, Fax: +44 (0)23 8051 1761, Email: h.m.haitchi@soton.ac.uk; JKW: Tel: +1 (774) 455-3784. Fax: +1 (508) 856-6696. Email: jonathan.watts@umassmed.edu

ABSTRACT

Two mechanisms dominate the clinical pipeline for oligonucleotide-based gene silencing, namely the antisense approach that recruits RNase H to cleave target RNA and the RNA interference (RNAi) approach that recruits the RISC complex to cleave target RNA. Multiple chemical designs can be used to elicit each pathway. We now compare the silencing of the asthma susceptibility gene *ADAM33* in MRC-5 lung fibroblasts using four different classes of gene silencing agents, two that use each mechanism: traditional duplex small interfering RNAs (siRNAs), single-stranded siRNAs (ss-siRNAs), Locked nucleic acid (LNA) gapmer antisense oligonucleotides (ASOs), and novel hexadecyloxypropyl conjugates of the ASOs. Of these designs, the gapmer ASOs emerged as lead compounds for silencing *ADAM33* expression: several gapmer ASOs showed subnanomolar potency when transfected with cationic lipid, and low micromolar potency with no toxicity when delivered gymnotically. The preferential susceptibility of *ADAM33* mRNA to silencing by RNase H may be related to the high degree of nuclear retention observed for this mRNA. Dynamic light scattering data showed that the hexadecyloxypropyl ASO conjugates self-assemble

into clusters. These conjugates showed reduced potency relative to unconjugated ASOs unless the lipophilic tail was conjugated to the ASO using a biocleavable linkage. Finally, based on the lead ASOs from (human) MRC-5 cells, we developed a series of homologous ASOs targeting mouse *Adam33* with excellent activity. Our work confirms that antisense oligonucleotide-based gene silencing of *ADAM33* is a useful tool for asthma research and therapy.

INTRODUCTION

Asthma is a chronic respiratory disease involving airway inflammation and structural changes in the form of remodeling of the conducting airways.[1-2] It causes over 345,000 deaths annually and affects over 340 million people worldwide.[3] A Disintegrin And Metalloprotease (*ADAM*) *33* is the first asthma susceptibility gene to be identified by positional cloning.[4] Single nucleotide polymorphisms in *ADAM33* have been linked to asthma and bronchial hyperresponsiveness.[4-5] *ADAM33* encodes a membrane-anchored metalloprotease, but a soluble metalloprotease-containing form of ADAM33 (sADAM33) is increased in bronchoalveolar lavage fluid of asthmatic patients.[6-7] Furthermore, in human embryonic lung explant culture, treatment with sADAM33 induces angiogenesis[8] and myogenesis,[7] pathological features of airway remodeling in asthma. Expression of human sADAM33 in transgenic mice causes pathological airway remodeling and makes airways more susceptible to allergen induced inflammatory responses.[7] Promisingly, when induction of human sADAM33 is arrested, this leads to reversal of the remodeling and reduced sensitivity to inflammatory responses.[7] Furthermore, in *Adam33*-null mice challenged with allergen, both airway remodeling and inflammation are suppressed. Therefore, inhibition of *ADAM33* represents an attractive disease-modifying therapeutic strategy for treating the root cause of asthma in many patients.

It is thus crucial to develop therapeutic agents capable of silencing of *ADAM33* expression. Since small molecule metalloprotease inhibitors have shown a poor specificity profile,[9] chemically optimized oligonucleotide-based inhibitors could serve as an excellent alternative.[10-12] In this study, we compared four types of oligonucleotide-based gene silencing agents for inhibition of *ADAM33/Adam33* (Figure 1): (i) duplex siRNAs, (ii) chemically modified single-stranded siRNAs (ss-siRNAs) that operate by the RISC pathway[13-14] (iii) LNA gapmer antisense oligonucleotides (ASOs) operating via the RNase H mechanism[15-17] and (iv) novel biocleavable lipid conjugates of the potent ASOs (including biocleavable conjugates). The LNA gapmers, delivered using cationic lipid or by gymnosis,[18]

provided significantly increased potency for silencing *ADAM33* relative to the siRNAs or ss-siRNAs.

RESULTS

ADAM33 silencing by siRNAs and ss-siRNAs

We designed and synthesized a panel of 13 duplex siRNAs targeting different regions of the *ADAM33* transcript (Figure 2A). We then tested the efficacy of these siRNAs in MRC-5 human lung fibroblast cells, transfecting the siRNAs with a lipid transfection reagent and measuring silencing by qPCR. We found that most of the sequences were inactive, while the most active duplexes were able to attain about 70% silencing (Figure 2B).

Single-stranded oligonucleotides can be recognized by the RNAi machinery and serve as guide strands, if the oligomer is stabilized to resist nuclease cleavage and contains a 5'-phosphate or phosphonate.[13-14, 19-20] To explore whether changing the biophysical properties of the RNAi trigger could improve activity, we synthesized and tested ss-siRNA analogues of three siRNA sequences: highly active sequence **HMH-1**, moderately active sequence **HP-2**, and inactive sequence **HP-3**. The ss-siRNA analogues showed reduced efficacy (**HMH1, HP-2**) or maintained inactivity (**HP-3**, Figure 2C). For the most active siRNA sequence **HMH-1**, we also carried out a chemical optimization of the ss-siRNAs and found one analogue with activity that was comparable but not superior to the parent duplex RNA (Figure 2D). Only the ss-siRNA with 2'OMe-RNA modifications at the 3'-terminus was able to approach the potency of the duplex siRNA (**ssi-HMH-1c**, Figure 2D). This result was followed up in the context of other sequences and targets, and this exploration of the medicinal chemistry of ss-siRNAs was recently published.[21] Overall, neither siRNAs nor ss-siRNAs were able to surpass 70% silencing of the *ADAM33* transcript under any of the conditions we tested.

To ensure that the relatively limited silencing we observed was not an artifact of either of the above designs, we also synthesized and tested a third option for siRNA design – i.e., fully chemically modified duplex siRNAs. We applied an alternating pattern of 2'OMe-RNA and 2'F-RNA to the HMH-1 sequence, using a 5'-phosphorylated 21-mer guide strand and a 15-nt sense strand (Supporting Figure S1). This and similar designs have been widely used and show excellent results both in vitro and in vivo.[22-26] The fully modified duplex was transfected into MRC-5 cells, and its efficacy was comparable to the parent unmodified siRNA duplex (Supporting Figure S1).

LNA gapmers show high potency when transfected with a cationic lipid

Another major class of single stranded gene silencing oligonucleotides are gapmer antisense oligonucleotides (ASOs).[27-29] Gapmer ASOs operate through a different mechanism than the siRNAs and ss-siRNAs above: they recruit RNase H to cleave target mRNAs.[30-32] The "wings" of gapmers are consist of sugar-modified nucleotides such as 2'-*O*-MOE-RNA[33] or LNA,[34-36] which increase binding affinity and nuclease stability, while the central "gap" is phosphorothioate DNA which elicits RNase H cleavage of the target. We designed and synthesized twelve phosphorothioate (PS) LNA gapmers, using a 3-9-3 pattern of sugars, targeting various regions of *ADAM33* mRNA (Figure 3A). We initially tested the LNA gapmers at 50nM concentration in MRC-5 fibroblasts, using Lipofectamine RNAiMAX as transfection agent. LNAs **33-G**, **33-N**, **33-O**, **33-P**, **33-Q**, and **33-R** all achieved >80% silencing of *ADAM33* when normalized to a scrambled siRNA duplex control (Figure 3B). This very high hit rate and maximal efficacy contrast sharply with the low hit rate and maximal efficacy observed when using RISC dependent oligonucleotides (siRNAs and ss-siRNAs) for this target. Furthermore, a dose response analysis shows potent, dose-dependent *ADAM33* inhibition for **33-O** and **33-R** to concentrations < 0.16nM (Figure 3C).

Gymnotic delivery of LNA gapmers

Although the LNA gapmers were highly potent in cultured cells, transfection efficiency *in vitro* does not always correlate well with *in vivo* studies. *Ex vivo* lung tissue and *in vivo* lung experiments also require oligonucleotides with the ability to exert potent silencing without the aid of toxic transfection agents. Naked LNA or 2'-fluoroarabinonucleic acid (2'F-ANA) ASOs can be taken up by most types of dividing cells in culture in a process termed "gymnosis".[37-39] Gymnotic delivery does not require serum additives or transfection reagents but is a slower process compared to lipofection. It tends to show low toxicity and shows an improved correlation between *in vitro* and *in vivo* results.[37]

The gymnotic approach was adopted to test (a) if the LNA gapmers could enter the MRC-5 cells without the use of transfection agents, (b) how the potency of the LNA gapmers delivered via gymnotic delivery compared to the transfections using a cationic lipid, and (c) whether the gymnotically delivered LNA gapmers were toxic to cultured cells.

A time course experiment was performed gymnotically delivering **33-O** into MRC-5 cells at a 1µM dose to determine the optimal day to harvest the cells after treatment, between day 4

and day 9. Our results indicate that day 7 post-treatment was an appropriate time to harvest cells (Supporting Figure S2). We then selected LNA gapmers **33-G**, **N**, **O**, **P**, and **R** for further testing. Oligomers **33-N**, **O**, and **P** achieved >80% reduction of *ADAM33* transcript levels, while **33-R** showed 60% *ADAM33* silencing at a 3µM dose (Figure 4).

The LNA gapmers are able to efficiently silence *ADAM33* expression without the aid of transfection agents. Although the potency of the gymnotically delivered oligonucleotides was not as high as the cationic lipid mediated LNA delivery, the gymnotically delivered LNAs showed no toxicity to cultured cells (based on phenotype and cell confluence).

Hexadecyloxypropyl conjugates for cellular uptake

One of the major limitations to oligonucleotides as therapeutic agents is their relatively poor uptake into most cells.[40] One promising solution is the covalent attachment of a ligand that allows recognition by cell-surface receptors.[41-43] We sought to improve uptake by attaching a lipid moiety based on 1-*O*-hexa-decyloxy-1,3-propanediol, which has been previously shown to increase small molecule uptake by MRC-5 fibroblast cells[44] and improve the oral bioavailability of nucleoside drugs.[45]

A 1-*O*-hexadecylpropanediol phosphoramidite was synthesized in two steps (Figure 5A). Treatment of propanediol in dimethylformamide with sodium hydride followed by addition of hexadecyl bromide and catalytic potassium iodide gave 1-*O*-hexadecyl-1,3,-propanediol in a single step as previously observed;[46] recrystallisation with hexane yielded white crystals of excellent purity. The phosphoramidite was synthesized under standard conditions using 2-cyanoethyloxy(*N,N*-diisopropylamino)phosphonamidic chloride. The phosphoramidite was then conjugated to the 5'-end of LNA gapmers **33-N**, **O**, and **P** via solid phase synthesis (Figure 5A).

Besides direct recognition of cell-surface receptors by conjugated small molecules, conjugation approaches may also change the biophysical properties of the oligonucleotide which may affect their cell uptake in a more indirect way. For example, a variety of amphiphilic oligonucleotide conjugates have been shown to assemble into micelle-type structures. Previous work has described very long polymer conjugates that induce self-assembly of oligonucleotides into clusters,[47] as well as oligonucleotides with shorter hydrophobic tails that assemble around a liposomal core.[48]

Therefore, we tested whether our conjugates self-assemble using dynamic light scattering. Indeed, we found that conjugation of a hexadecyloxypropyl tail clearly induced assembly of oligonucleotides into clusters (Figure 5B). Our work demonstrates that even a simple

hydrophobic conjugate may be sufficient to induce efficient self-assembly into clusters/micelles.

Clustering/assembly of oligonucleotides often correlates with enhanced uptake and activity, across multiple size scales and likely via multiple mechanisms.[49-50] Nevertheless, in our case in spite of the efficient self-assembly observed for the lipid tail conjugates, the biostable hexadecyloxypropyl conjugates showed reduced silencing efficacy in cells (Figure 5C). A highly lipophilic tail might lead to stronger association with cell membranes but fail to release active oligonucleotide into the cytoplasm.[51] We therefore generated biocleavable analogues based on a section of phosphodiester (PO)-linked DNA between the lipid tail and the phosphorothioate (PS) gapmer ASO (Figure 5A). Nuclease cleavage at the PO linkages would allow release of the gapmer from the lipid tail inside endosomes.[52] We found that treatment of cells with these biocleavable constructs produced similar potency silencing of *ADAM33* relative to the analogous unconjugated gapmers, but did not provide a potency advantage *in vitro* (Figure 5C). However, hydrophobic conjugates of gapmer oligonucleotides may provide an advantage for tissue distribution or other *in vivo* properties, and our data point to the importance of making hydrophobic conjugates in a biocleavable manner, to avoid any membrane entrapment and associated potency reduction.

ASOs designed to homologous regions of the mouse *Adam33* transcript are also active

To explore the biological role of *ADAM33* / *Adam33* in asthma progression, we have developed a series of mouse models.[7] We therefore set out to identify analogues of the human lead ASOs that could silence mouse *Adam33* expression. The mouse and human *ADAM33* / *Adam33* transcripts are relatively well conserved in the coding region, but diverge substantially toward the 3'-end of the ORF and in their 3'-UTR sequences (for example, the mouse transcript has a much shorter UTR sequence than the human transcript).

Two of our active ASOs targeting the human *ADAM33* transcript also had significant sequence homology to the mouse transcript (G and N, Table 1). While the sequence conservation in the 3'-UTR was very poor, we also did an analysis of the conservation of structural features using T-coffee,[53] and designed targets to regions of conserved structure (P and Q, near the end of the ORF, and R, in the 3'-UTR, Table 1). These five sequences were synthesized as 3-9-3 LNA gapmers and tested for their ability to inhibit *Adam33* expression in mouse embryonic fibroblasts (Figure 6).

The most active ASOs in terms of silencing mouse *Adam33* expression were those targeting the 3'-end of the ORF or the 3'-UTR (Figure 6), which were also the three sequences that

were less well conserved relative to the human hits. In future studies, we will test these sequences in mouse models to further explore the role of *ADAM33* / *Adam33* in asthma, and the potential for oligonucleotides to play a therapeutic role in its treatment.

DISCUSSION

Single-stranded oligonucleotides are amenable to simple delivery approaches (including free uptake by simply delivering naked oligonucleotides into the blood or the CNS) and this fact has led to a significant drive to develop single-stranded oligonucleotides, including fully[13-14] or partly[23-24] single-stranded oligomers that can engage the RNAi machinery (RISC). These are appropriate for gene silencing applications where recruitment of RISC is required – for example, in the context of allele-selective silencing of mutant Huntingtin, RISC-dependent approaches showed far greater selectivity (>30-fold)[13, 54-55] compared with simpler steric blocker ASOs (~3-6 fold).[56-57]

However, for silencing nuclear-localized transcripts, recruitment of RISC may not be ideal. *ADAM33* mRNA is ~90% nuclear-localized in spite of the fact that it is a protein-coding transcript.[58] RNase H is predominantly localized in the nucleus,[59] and plays a role in genome defense including elimination of R-loops.[60] After gapmer-induced RNase H cleavage of a target RNA, the 3'-fragment is predominantly degraded by the nuclear enzyme 5'-3' exoribonuclease 2 (XRN2).[61] Nuclear RNAs including intronic sequences are very vulnerable to cleavage induced by gapmer ASOs,[62-64] and in the context of noncoding RNAs, it was recently observed that ASOs are less sensitive to subcellular localization of their targets while siRNAs tend to be more effective at silencing ncRNAs that are predominantly cytoplasmic.[65] This empirical tendency exists in spite of the fact that a cytoplasmic mechanism has also recently been described for gapmer ASO action,[66] and that RNAi factors are present and active in human cell nuclei.[67] Our current study suggests that it is important to consider subcellular localization of the target when selecting a preferred oligonucleotide class for silencing, even if the target is a protein-coding mRNA.

Our results should not be taken as a statement about the relative value or potency of ASO and siRNA silencing in general. For many targets, particularly in vitro, it is easier to find potent siRNAs than potent ASOs. The siRNA–Argonaute and ASO–RNase H approaches should be considered complementary rather than redundant.

In this current project, multiple RNase H-dependent LNA gapmers were highly effective silencing agents for *ADAM33* mRNA while siRNAs failed to yield potent silencing. Since gymnotically delivered oligonucleotides showed no toxicity and high efficiency in cultured

cells, they are ideal for further *ADAM33* studies. We are exploring the delivery of anti-*Adam33* oligonucleotides to mouse airways and the therapeutic potential of ASO-mediated inhibition of *ADAM33* for reversing pathological airway remodeling in asthma and other chronic lung diseases including COPD[68-69] and sarcoidosis.[70]

MATERIALS AND METHODS

General methods

^{1}H, ^{13}C, ^{31}P NMR spectra were recorded on Bruker DPX or Bruker AV NMR spectrometers operating at 400, 101 and 162 MHz respectively. Small molecules were analyzed using a Waters (Manchester, UK) TQD mass spectrometer equipped with a triple quadrupole analyzer. Samples were introduced to the mass spectrometer via an Acquity UPC^2 system including a UPC^2 Waters HSS C18 SB column (100 mm x 3.0 mm 1.8µm) Gradient 90% CO_2:10% methanol modifier (25mM ammonium acetate) to 60% CO_2:40% methanol modifier (25mM ammonium acetate) in 3 min at a flow rate of 1.5 mL/min. The make-up flow (methanol / 1% formic acid) was pumped at a flow rate of 0.45mL/min into the mass spectrometer. Mass spectra were recorded using positive ion electrospray ionization.

Oligonucleotides

siRNAs were designed using the Whitehead siRNA selection server (http://sirna.wi.mit.edu). ASOs were manually designed using the predicted secondary structure of the mRNA (from mFold[71]), the predicted self-structure of the oligonucleotide, and the predicted specificity (from NCBI BLAST).

The first set of siRNAs for sequence screening was purchased from Integrated DNA Technologies. All other oligonucleotides were synthesized in-house at a 1 µmol scale on Applied Biosystems 394 DNA/RNA synthesizers with Unylinker (ChemGenes) or nucleoside-loaded CPG supports and standard detritylation and capping reagents. Activation was achieved with 5-Benzylthio-1H-Tetrazole (BTT, 0.3M in acetonitrile). Oxidation was achieved using 0.02 M iodine in THF/water/pyridine. Sulfurization was accomplished with the 1,2,4-dithiazolines EDITH (Link Technologies) or DDTT (0.1M, ChemGenes). RNA, 2'F-RNA and 2'OMe-RNA phosphoramidites (ChemGenes) were dissolved to a concentration of 0.15M in anhydrous acetonitrile immediately prior to use. LNA and MOE phosphoramidites were synthesized by standard methods[33, 72-73] from 3'-hydroxyl precursors (Rasayan) using 2-cyanoethyloxy(*N,N*-diisopropylamino)phosphonamidic chloride and were used at 0.1 or 0.15 M in acetonitrile, with the exception of LNA 5-MeC (all "LNA-C" is actually LNA 5-Me-C)

which was dissolved in a 3:1 mixture of THF:acetonitrile. Coupling times for all modified phosphoramidites were 10 minutes. Coupling yields for all nucleoside phosphoramidites were >98%. Coupling yields for the hexadecyloxypropyl phosphoramidite were very good as long as the quality of the phosphoramidite was excellent. When during one experiment we used a batch of hexadecyloxypropyl phosphoramidite with somewhat lower purity, the coupling yield dropped to 50%.

Unmodified RNA was deprotected using a 3:1 ratio of NH_4OH/ EtOH for 48 hours at room temperature. The RNA 2'OH tert-butyldimethylsilyl protecting group was removed with a 4:1 DMSO / TEA·3HF solution at 65ºC for 3 hours. The reaction was cooled to room temperature then precipitated by the addition of 3M NaOAc (25 μL) and BuOH (1 mL). The mixture was centrifuged at 4ºC for 5 minutes at 8000 rpm, washed with 70% EtOH, air dried, and the pellet was resuspended in RNase-free water. 2'-modified RNA, LNA and DNA were deprotected with concentrated NH_4OH at 55ºC overnight.

Oligonucleotides were evaporated to dryness by rotary evaporation then resuspended in 1mL RNase-free water. If LCMS and analytical PAGE (see below) indicated that the oligomer was sufficiently pure, it was desalted with a Nap-10 column (GE Healthcare) and used directly. All oligonucleotides were characterized on Bruker MicrOTOF Ultimate 3000 or Agilent Q-TOF LCMS systems with electrospray ionization and time of flight analysis, using negative ionization mode. All sequences and mass spectrometric data are provided in Supporting Tables S1-S5.

20μM working stocks of siRNAs were prepared by annealing the sense and antisense strands in a final 2.5x PBS buffer. The solutions were heated at 95ºC for 10 minutes and then cooled to room temperature at a rate of 1ºC per minute.

Oligonucleotide purification and electrophoresis

Approximately 20 A_{260} units (preparative gel) or 0.1 A_{260} units (analytical gel) was loaded into a 20% polyacrylamide gel containing 7M urea and run at 400V for ~3 hours. Analytical gels were visualized using Stains-All (Sigma). For preparative gels, the product band was briefly visualized by UV shadowing, excised from the gel and incubated in RNase-free water overnight. The aqueous solution was then concentrated by rotary evaporator, resuspended in RNase-free water, and desalted via a Nap-25 column (GE Healthcare). The desalted oligonucleotide was evaporated to dryness again and resuspended in a small volume of RNase-free water.

Hexadecyloxypropyl-conjugated oligonucleotides were purified by 20% denaturing PAGE as above, or by ion exchange chromatography using an Agilent 1200-series HPLC, an Agilent PL-SAX column, and eluents containing 30% aqueous acetonitrile with increasing sodium perchlorate. Either method allowed us to remove all unconjugated oligonucleotide and obtain the pure conjugate.

Cell culture and transfection

MRC-5 embryonic fibroblasts were maintained at 37ºC and 5% CO_2 in DMEM supplemented with 10% FBS, 2% L-Glutamine, 1% NEAA, and 1% sodium pyruvate (all from Sigma). Cells were plated in 6-well plates at 150k cells/well (cationic lipid) or 25k cell/well (gymnotic) 24 hours prior to transfection, unless otherwise stated. Mouse embryonic fibroblasts (MEFs) were maintained in DMEM supplemented with 10% FBS and were plated in 6-well plates at 100k cells/well 24 hours prior to transfection.

Oligonucleotides were transfected at 50nM concentration for single dose or decreasing doses for dose responses. Cells were transfected using RNAiMAX (Life Technologies) using 0.75µL lipid per 1µL of oligonucleotide (siRNA) or 0.67 µL per 1 µL oligonucleotide (LNA) in OptiMEM (Life Technologies). Gymnotic delivery was achieved using 1 µM or 3 µM oligonucleotide concentration in full cell culture media. Cells were harvested for RNA analysis 3 days after transfection (lipid) or 7 days post treatment (gymnotic) unless otherwise stated.

RNA harvest and Quantitative real-time PCR (qRT-PCR)

Total RNA from cells was harvested 3 days post transfection (lipid transfection) or 7 days post transfection (gymnotic) unless otherwise stated. After washing each well with 1mL PBS, 1mL of RiboZol (Amresco) was added to each well, incubated for 2 min at room temperature and transferred to 1.5-mL microcentrifuge tube. Chloroform (200µL) was added to each tube and the mixture was shaken vigorously for 1 minute then incubated at room temperature for 10 minutes. The mixture was centrifuged at 13,000 rpm for 20 min, then the clear aqueous layer was transferred to a new 1.5-mL tube, avoiding any interphase. 2-propanol (600µL) was added to the aqueous layer followed by a 1-min vigorous shake then a 20-min incubation at -20ºC followed by a 15-min centrifugation at 14k rpm at 4 ºC. The resulting pellet was washed with ice cold 70% ethanol, re-centrifuged at 8000 rpm for 10 min at 4 ºC, and then briefly allowed to air dry. The pellet was resuspended in RNase-free water, heated to 55ºC for 5 min, then was quantitated by UV spectroscopy.

1 µg of RNA was treated with 2 units of DNase I (Worthington Biochemical Corporation) for 10 min at 37ºC followed by 10 min at 75ºC. RNA was reverse transcribed using a High Capacity cDNA Reverse Transcription Kit (Life Technologies) per manufacturer's protocol.

qRT-PCR was performed using iTaq Supermix (BioRad) on a BioRad CFX96 real time system. Data were normalized relative to levels of *GAPDH* mRNA. A primer/probe assay (IDT) specific for the *ADAM33* 3'-untranslated region was used (unless otherwise stated): forward primer, 5'-GGCCTCTGCAAACAAACATAATT-3'; reverse primer, 5'-GGGCTCAGGAACCACCTAGG-3'; probe, 5'-CTTCCTGTTTCTTCCCACCCTGTCTTCTCT-3'. GAPDH primer/probe assay (IDT); forward primer, 5'-TGGTCCAGGGGTCTTACT-3'; reverse primer, 5'-CCTCAACGACCACTTTGT-3'; probe, 5'-CTCATTTCCTGGTATGACAACGAATTTGGC-3'. For mouse *Adam33* mRNA quantitation, we used TaqMan (ThermoFisher) probe set Mm00459697_g1. All qRT-PCR experiments were performed in technical replicates. The qRT-PCR cycle was as follows: 95℃ for 7 minutes; (95℃ for 15 seconds; 60℃ for 30 seconds) x 40 cycles.

Dynamic light scattering

The lyophilized gapmer ASO (**33-O**) and its hexadecyloxypropyl conjugate (**33-O** biostable conjugate) were dissolved in RNase-free water at a concentration of 20 nM and filtered with 0.2 um filter prior to measurement. The filtered samples were then transferred to a 384-well microplate and placed into a DynaPro PlateReader-II system (WYATT Technology) for DLS measurement. The data was collected by averaging 10 measurements (~5 s each) for each sample.

2-cyanoethyl (3-(hexadecyloxy)propyl) diisopropylphosphoramidite

3-(Hexadecyloxy)propan-1-ol was synthesized in one step according to the method of Yamano et al[46] and recrystallized from hexane. The crystalline product (200mg, 0.67mmol) was dissolved in dry CH_2Cl_2 and diisopropylethylamine (0.70 mL, 2.68 mmol, 4 equiv) was added while stirring at RT. 2-Cyanoethyloxy(N,N-diisopropylamino) phosphonamidic chloride (0.18mL, 0.8mmol, 1.2 eq) was added dropwise and the solution was stirred for 45min. After completion 15mL of CH_2Cl_2 were added and the organic phase was washed with saturated aqueous $NaHCO_3$ and dried over $MgSO_4$. The crude product was purified on a silica column with Hex:EtOAc:NEt_3 50:50:1 as eluent to afford the title compound as a colorless liquid (175mg, 52% yield).) R_f in EtOAc =0.28. MS (ESI): found 501 (M+H); mass expected for ($C_{28}H_{57}N_2O_3P$ + H = 501.4). ^{1}H NMR (400 MHz, $CDCl_3$) δ 0.89 (t, *J*=6.85 Hz, 3H, $C\underline{H}_3CH_2$) 1.19 (dd, *J*=6.72, 3.42 Hz, 12H, 2 $(C\underline{H}_3)_2CHN$) 1.26 (s, 26 H, 13 $(C\underline{H}_2)_n$) 1.56 (quin, *J*=6.94 Hz, 2H, $OCH_2C\underline{H}_2CH_2$) 1.88 (quin, *J*=6.30 Hz, 2H, $POCH_2C\underline{H}_2CH_2O$) 2.64 (t, *J*=6.60 Hz, 2H,

$C\underline{H_2}CN$) 3.40 (t, *J*=6.66 Hz, 2H, $OC\underline{H_2}CH_2CH_2$) 3.50 (t, *J*=6.30 Hz, 2H, $POCH_2CH_2C\underline{H_2}O$) 3.54 - 3.65 (m, 2H, 2 C<u>H</u>) 3.65 - 3.79 (m, 2H, $POC\underline{H_2}CH_2CH_2O$) 3.79 - 3.93 ppm (m, 2H, $POC\underline{H_2}CH_2CN$). ^{13}C NMR (101 MHz, $CDCl_3$) δ 14.1 (s, 1C, $\underline{C}H_3CH_2$) 20.3 (d, *J*=6.60 Hz, 1C, $\underline{C}H_2CN$) 22.7 (s, 1C, $CH_2\underline{C}H_2CH_3$) 24.5 and 24.63 (2 d, *J*=7.70 Hz, 2x2C, $(\underline{C}H_3)_2CHN$) 26.2 (s, 1C, $OCH_2CH_2\underline{C}H_2$) 29.3 (s, $1CH_{2n}$) 29.5 (s, $1CH_{2n}$) 29.6 (s, $2CH_{2n}$) 29.6 (s, $1CH_{2n}$) 29.7 (s, $5CH_{2n}$) 29.8 (s, $1CH_{2n}$) 31.5 (d, *J*=7.34 Hz, 1C, $POCH_2\underline{C}H_2CH_2O$) 31.9 (s, $1CH_{2n}$) 43.0 (d, *J*=11.74 Hz, 2C, 2 <u>C</u>H) 58.3 (d, *J*=19.07 Hz, 1C, $PO\underline{C}H_2CH_2CN$) 60.7 (d, *J*=17.61 Hz, 1C, $PO\underline{C}H_2CH_2CH_2O$) 67.3 (s, 1C, $POCH_2CH_2\underline{C}H_2O$) 71.1 (s, 1C, $O\underline{C}H_2CH_2CH_2$), 117.6 ppm (s, 1C, <u>C</u>N). ^{31}P NMR (162 MHz, $CDCl_3$, ^1H-decoupled) δ 147.56 ppm (s).

ACKNOWLEDGEMENTS

We thank Dr Neil Wells for help establishing ^{31}P NMR protocols. We are also very grateful to Dr Dorcas Brown and ATDBio for support with oligonucleotide synthesis while we were at the University of Southampton. This work was supported by a pilot project grant by the Institute for Life Sciences (University of Southampton) to JKW and HMH, by UMass Medical School startup funds to JKW, and by the Engineering and Physical Sciences Research Council [EP/M003973/1 to JKW]. HMH was supported by a Medical Research Council (MRC) Clinician Scientist Fellowship G0802804.

REFERENCES

1. Koppelman, G. H.; Sayers, I., (2011). Evidence of a genetic contribution to lung function decline in asthma. *J. Allergy Clin. Immunol.* **128:** 479-484.
2. Tang, M. L. K.; Wilson, J. W.; Stewart, A. G.; Royce, S. G., (2006). Airway remodelling in asthma: Current understanding and implications for future therapies. *Pharmacol. Ther.* **112:** 474-488.
3. Global Asthma Network *The Global Asthma Report*; 2014; p globalasthmareport.org.
4. Eerdewegh, P. V., et al. , (2002). Association of the ADAM33 gene with asthma and bronchial hyperresponsiveness. *Nature* **418:** 426-430.
5. Lee, J. H.; Park, H. S.; Park, S. W.; Jang, A. S.; Uh, S. T.; Rhim, T.; Park, C. S.; Hong, S. J.; Holgate, S. T.; Holloway, J. W.; Shin, H. D., (2004). ADAM33 polymorphism: association with bronchial hyper-responsiveness in Korean asthmatics. *Clin. Exp. Allergy* **34:** 860-865.
6. Lee, J. Y.; Park, S. W.; Chang, H. K.; Kim, H. Y.; Rhim, T. Y.; Lee, J. H.; Jang, A. S.; Koh, E. S.; Park, C. S., (2006). A disintegrin and metalloproteinase 33 protein in patients with asthma - Relevance to airflow limitation. *Am. J. Respir. Crit. Care Med.* **173:** 729-735.
7. Davies, E. R.; Kelly, J. F. C.; Howarth, P. H.; Wilson, D. I.; Holgate, S. T.; Davies, D. E.; Whitsett, J. A.; Haitchi, H. M., (2016). Soluble ADAM33 initiates airway remodeling to promote susceptibility for allergic asthma in early life. *JCI Insight* **1:** e87632.
8. Puxeddu, I.; Pang, Y. Y.; Harvey, A.; Haitchi, H. M.; Nicholas, B.; Yoshisue, H.; Ribatti, D.; Clough, G.; Powell, R. M.; Murphy, G.; Hanley, N. A.; Wilson, D. I.; Howarth, P. H.; Holgate, S. T.; Davies, D. E., (2008). The soluble form of a disintegrin and metalloprotease 33 promotes

angiogenesis: Implications for airway remodeling in asthma. *Journal of Allergy and Clinical Immunology* **121:** 1400-1406.
9. Coussens, L. M.; Fingleton, B.; Matrisian, L. M., (2002). Matrix metalloproteinase inhibitors and cancer: trials and tribulations. *Science* **295:** 2387-92.
10. Khvorova, A.; Watts, J. K., (2017). The chemical evolution of oligonucleotide therapies of clinical utility. *Nat. Biotechnol.* **35:** 238-248.
11. Sharma, V. K.; Watts, J. K., (2015). Oligonucleotide therapeutics: chemistry, delivery and clinical progress. *Future medicinal chemistry* **7:** 2221-42.
12. Deleavey, G. F.; Damha, M. J., (2012). Designing chemically modified oligonucleotides for targeted gene silencing. *Chem. Biol.* **19:** 937-54.
13. Yu, D.; Pendergraff, H.; Liu, J.; Kordasiewicz, H. B.; Cleveland, Don W.; Swayze, Eric E.; Lima, Walt F.; Crooke, Stanley T.; Prakash, Thazha P.; Corey, David R., (2012). Single-Stranded RNAs Use RNAi to Potently and Allele-Selectively Inhibit Mutant Huntingtin Expression. *Cell* **150:** 895-908.
14. Lima, Walt F.; Prakash, Thazha P.; Murray, Heather M.; Kinberger, Garth A.; Li, W.; Chappell, Alfred E.; Li, Cheryl S.; Murray, Susan F.; Gaus, H.; Seth, Punit P.; Swayze, Eric E.; Crooke, Stanley T., (2012). Single-Stranded siRNAs Activate RNAi in Animals. *Cell* **150:** 883-894.
15. Wahlestedt, C.; Salmi, P.; Good, L.; Kela, J.; Johnsson, T.; Hokfelt, T.; Broberger, C.; Porreca, F.; Lai, J.; Ren, K. K.; Ossipov, M.; Koshkin, A.; Jakobsen, N.; Skouv, J.; Oerum, H.; Jacobsen, M. H.; Wengel, J., (2000). Potent and nontoxic antisense oligonucleotides containing locked nucleic acids. *Proc. Natl. Acad. Sci. USA* **97:** 5633-5638.
16. Kurreck, J.; Wyszko, E.; Gillen, C.; Erdmann, V. A., (2002). Design of antisense oligonucleotides stabilized by locked nucleic acids. *Nucleic Acids Res.* **30:** 1911-1918.
17. Fluiter, K.; Mook, O. R. F.; Vreijling, J.; Langkjaer, N.; Hojland, T.; Wengel, J.; Baas, F., (2009). Filling the gap in LNA antisense oligo gapmers: the effects of unlocked nucleic acid (UNA) and 4 '-C-hydroxymethyl-DNA modifications on RNase H recruitment and efficacy of an LNA gapmer. *Mol. Biosyst.* **5:** 838-843.
18. Stein, C. A.; Hansen, J. B.; Lai, J.; Wu, S.; Voskresenskiy, A.; Hog, A.; Worm, J.; Hedtjarn, M.; Souleimanian, N.; Miller, P.; Soifer, H. S.; Castanotto, D.; Benimetskaya, L.; Orum, H.; Koch, T., (2010). Efficient gene silencing by delivery of locked nucleic acid antisense oligonucleotides, unassisted by transfection reagents. *Nucleic Acids Res* **38:** e3.
19. Kini, H. K.; Walton, S. P., (2007). In vitro binding of single-stranded RNA by human Dicer. *FEBS Lett.* **581:** 5611-6.
20. Holen, T.; Amarzguioui, M.; Babaie, E.; Prydz, H., (2003). Similar behaviour of single-strand and double-strand siRNAs suggests they act through a common RNAi pathway. *Nucleic Acids Res.* **31:** 2401-2407.
21. Pendergraff, H. M.; Debacker, A. J.; Watts, J. K., (2016). Single-Stranded Silencing RNAs: Hit Rate and Chemical Modification. *Nucleic Acid Ther* **26:** 216-22.
22. Allerson, C. R.; Sioufi, N.; Jarres, R.; Prakash, T. P.; Naik, N.; Berdeja, A.; Wanders, L.; Griffey, R. H.; Swayze, E. E.; Bhat, B., (2005). Fully 2'-Modified Oligonucleotide Duplexes with Improved in Vitro Potency and Stability Compared to Unmodified Small Interfering RNA. *J. Med. Chem.* **48:** 901-904.
23. Byrne, M.; Tzekov, R.; Wang, Y.; Rodgers, A.; Cardia, J.; Ford, G.; Holton, K.; Pandarinathan, L.; Lapierre, J.; Stanney, W.; Bulock, K.; Shaw, S.; Libertine, L.; Fettes, K.; Khvorova, A.; Kaushal, S.; Pavco, P., (2013). Novel hydrophobically modified asymmetric RNAi compounds (sd-rxRNA) demonstrate robust efficacy in the eye. *J. Ocul. Pharmacol. Ther.* **29:** 855-864.
24. Alterman, J. F.; Hall, L. M.; Coles, A. H.; Hassler, M. R.; Didiot, M. C.; Chase, K.; Abraham, J.; Sottosanti, E.; Johnson, E.; Sapp, E.; Osborn, M. F.; Difiglia, M.; Aronin, N.; Khvorova, A., (2015). Hydrophobically Modified siRNAs Silence Huntingtin mRNA in Primary Neurons and Mouse Brain. *Mol. Ther. Nucl. Acids* **4:** e266.
25. Nikan, M.; Osborn, M. F.; Coles, A. H.; Biscans, A.; Godinho, B. M. D. C.; Haraszti, R. A.; Sapp, E.; Echeverria, D.; DiFiglia, M.; Aronin, N.; Khvorova, A., (2017). Synthesis and Evaluation of

Parenchymal Retention and Efficacy of a Metabolically Stable O-Phosphocholine-N-docosahexaenoyl-l-serine siRNA Conjugate in Mouse Brain. *Bioconjugate Chem.* in press, DOI 10.1021/acs.bioconjchem.7b00226.

26. Fitzgerald, K.; White, S.; Borodovsky, A.; Bettencourt, B. R.; Strahs, A.; Clausen, V.; Wijngaard, P.; Horton, J. D.; Taubel, J.; Brooks, A.; Fernando, C.; Kauffman, R. S.; Kallend, D.; Vaishnaw, A.; Simon, A., (2017). A Highly Durable RNAi Therapeutic Inhibitor of PCSK9. *N. Engl. J. Med.* **376:** 41-51.

27. Monia, B. P.; Lesnik, E. A.; Gonzalez, C.; Lima, W. F.; McGee, D.; Guinosso, C. J.; Kawasaki, A. M.; Cook, P. D.; Freier, S. M., (1993). Evaluation of 2'-modified oligonucleotides containing 2'-deoxy gaps as antisense inhibitors of gene expression. *J. Biol. Chem.* **268:** 14514-14522.

28. Inoue, H.; Hayase, Y.; Iwai, S.; Ohtsuka, E., (1987). Sequence-dependent hydrolysis of RNA using modified oligonucleotide splints and RNase H. *FEBS Lett.* **215:** 327-30.

29. Agrawal, S.; Zhang, X.; Lu, Z.; Zhao, H.; Tamburin, J. M.; Van, J.; Cai, H.; Diasio, R. B.; Habus, I.; Jiang, Z., (1995). Absorption, tissue distribution and in vivo stability in rats of a hybrid antisense oligonucleotide following oral administration. *Biochem. Pharmacol.* **50:** 571-576.

30. Juliano, R. L.; Ming, X.; Carver, K.; Laing, B., (2014). Cellular Uptake and Intracellular Trafficking of Oligonucleotides: Implications for Oligonucleotide Pharmacology. *Nucl. Acid Ther.* **24:** 101-113.

31. Bennet, C. F.; Swayze, E. E., (2010). RNA Targeting Therapeutics: Molecular Mechanisms of Antisense Oligonucleotides as a Therapeutic Platform. *Annu. Rev. Pharmacol. Toxicol* **50:** 259-93.

32. Watts, J. K.; Corey, D. R., (2012). Silencing disease genes in the laboratory and the clinic. *J. Pathol.* **226:** 365-379.

33. Martin, P., (1995). A New Access to 2'-*O*-Alkylated Ribonucleosides and Properties of 2'-*O*-Alkylated Oligoribonucleotides. *Helv. Chim. Acta* **78:** 486-504.

34. Singh, S. K.; Nielsen, P.; Koshkin, A. A.; Wengel, J., (1998). LNA (locked nucleic acids): synthesis and high-affinity nucleic acid recognition. *Chem. Commun.* 455-456.

35. Obika, S.; Nanbu, D.; Hari, Y.; Andoh, J.-i.; Morio, K.-i.; Doi, T.; Imanishi, T., (1998). Stability and structural features of the duplexes containing nucleoside analogues with a fixed N-type conformation, 2'-O,4'-C-methyleneribonucleosides. *Tetrahedron Lett.* **39:** 5401-5404.

36. Watts, J. K., (2013). Locked Nucleic Acid: Tighter is Different. *Chem Commun* **49:** 5618-1520.

37. Stein, C. A.; Hansen, J. B.; Lai, J.; Wu, S.; Voskresenskiy, A.; Hog, A.; Worm, J.; Hedtjarn, M.; Souleimanian, N.; Miller, P.; Soifer, H. S.; Castanotto, D.; Benimetskaya, L.; Orum, H.; Koch, T., (2010). Efficient gene silencing by delivery of locked nucleic acid antisense oligonucleotides, unassisted by transfection reagents. *Nucleic Acids Res.* **38**.

38. Souleimanian, N.; Deleavey, G. F.; Soifer, H.; Wang, S.; Tiemann, K.; Damha, M. J.; Stein, C. A., (2012). Antisense 2 '-Deoxy, 2 '-Fluoroarabino Nucleic Acid (2 ' F-ANA) Oligonucleotides: In Vitro Gymnotic Silencers of Gene Expression Whose Potency Is Enhanced by Fatty Acids. *Molecular Therapy-Nucleic Acids* **1:** 1-9.

39. Soifer, H. S.; Koch, T.; Lai, J.; Hansen, B.; Hoeg, A.; Oerum, H.; Stein, C. A., Silencing of Gene Expression by Gymnotic Delivery of Antisense Oligonucleotides. In *Functional Genomics: Methods and Protocols, Second Edition*, Kaufmann, M.; Klinger, C., Eds. Humana Press Inc: Totowa, 2012; Vol. 815, pp 333-346.

40. Winkler, J., (2013). Oligonucleotide conjugates for therapeutic applications. *Ther. Deliv.* **4:** 791-809.

41. Wolfrum, C.; Shi, S.; Jayaprakash, K. N.; Jayaraman, M.; Wang, G.; Pandey, R. K.; Rajeev, K. G.; Nakayama, T.; Charrise, K.; Ndungo, E. M.; Zimmermann, T.; Koteliansky, V.; Manoharan, M.; Stoffel, M., (2007). Mechanisms and optimization of in vivo delivery of lipophilic siRNAs. *Nat. Biotechnol.* **25:** 1149-1157.

42. Hostetler, K. Y.; Rybak, R. J.; Beadle, J. R.; Gardner, M. F.; Aldern, K. A.; Wright, K. N.; Kern, E. R., (2001). In vitro and in vivo activity of 1-O-hexadecylpropane-diol-3-phospho-ganciclovir and 1-O-hexadecylpropane-diol-3-phospho-penciclovir in cytomegalovirus and herpes simplex virus infections. *Antiviral Chem. Chemother.* **12:** 61-70.

43. Prakash, T. P.; Graham, M. J.; Yu, J.; Carty, R.; Low, A.; Chappell, A.; Schmidt, K.; Zhao, C.; Aghajan, M.; Murray, H. F.; Riney, S.; Booten, S. L.; Murray, S. F.; Gaus, H.; Crosby, J.; Lima, W. F.; Guo, S.; Monia, B. P.; Swayze, E. E.; Seth, P. P., (2014). Targeted delivery of antisense oligonucleotides to hepatocytes using triantennary N-acetyl galactosamine improves potency 10-fold in mice. *Nucleic Acids Res.* **42:** 8796-807.
44. Aldern, K. A.; Ciesla, S. L.; Winegarden, K. L.; Hostetler, K. Y., (2003). Increased antiviral activity of 1-O-hexadecyloxypropyl- 2-C-14 cidofovir in MRC-5 human lung fibroblasts is explained by unique cellular uptake and metabolism. *Mol. Pharmacol.* **63:** 678-681.
45. Hostetler, K. Y., (2009). Alkoxyalkyl prodrugs of acyclic nucleoside phosphonates enhance oral antiviral activity and reduce toxicity: Current state of the art. *Antiviral Res.* **82:** A84-A98.
46. Yamano, Y.; Tsuboi, K.; Hozaki, Y.; Takahashi, K.; Jin, X.-H.; Ueda, N.; Wada, A., (2012). Lipophilic amines as potent inhibitors of N-acylethanolamine-hydrolyzing acid amidase. *Biorg. Med. Chem.* **20:** 3658-3665.
47. Edwardson, T. G.; Carneiro, K. M.; Serpell, C. J.; Sleiman, H. F., (2014). An efficient and modular route to sequence-defined polymers appended to DNA. *Angew. Chem. Int. Ed. Engl.* **53:** 4567-71.
48. Banga, R. J.; Chernyak, N.; Narayan, S. P.; Nguyen, S. T.; Mirkin, C. A., (2014). Liposomal Spherical Nucleic Acids. *Journal of the American Chemical Society* **136:** 9866-9869.
49. Ezzat, K.; Aoki, Y.; Koo, T.; McClorey, G.; Benner, L.; Coenen-Stass, A.; O'Donovan, L.; Lehto, T.; Garcia-Guerra, A.; Nordin, J.; Saleh, A. F.; Behlke, M.; Morris, J.; Goyenvalle, A.; Dugovic, B.; Leumann, C.; Gordon, S.; Gait, M. J.; El-Andaloussi, S.; Wood, M. J., (2015). Self-Assembly into Nanoparticles Is Essential for Receptor Mediated Uptake of Therapeutic Antisense Oligonucleotides. *Nano Lett.* **15:** 4364-73.
50. Subramanian, R. R.; Wysk, M. A.; Ogilvie, K. M.; Bhat, A.; Kuang, B.; Rockel, T. D.; Weber, M.; Uhlmann, E.; Krieg, A. M., (2015). Enhancing antisense efficacy with multimers and multi-targeting oligonucleotides (MTOs) using cleavable linkers. *Nucleic Acids Res* **43:** 9123-32.
51. Nishina, T.; Numata, J.; Nishina, K.; Yoshida-Tanaka, K.; Nitta, K.; Piao, W.; Iwata, R.; Ito, S.; Kuwahara, H.; Wada, T.; Mizusawa, H.; Yokota, T., (2015). Chimeric Antisense Oligonucleotide Conjugated to alpha-Tocopherol. *Mol. Ther. Nucl. Acids* **4:** e220.
52. Lindholm, M. W.; Pendergraff, H.; Ravn, J.; Kammler, S.; Albaek, N., Getting LNAs to where they need to be: conjugation and linker strategies. In *12th annual meeting of the Oligonucleotide Therapeutics Society*, Montreal, Canada, 2016.
53. Notredame, C.; Higgins, D. G.; Heringa, J., (2000). T-Coffee: A Novel Method for Fast and Accurate Multiple Sequence Alignment. *J. Mol. Biol.* **302:** 205-217.
54. Hu, J.; Liu, J.; Corey, D., (2010). Allele-selective inhibition of huntingtin expression by switching to an miRNA-like RNAi mechanism. *Chem Biol* **17:** 1183-8.
55. Fiszer, A.; Mykowska, A.; Krzyzosiak, W. J., (2011). Inhibition of mutant huntingtin expression by RNA duplex targeting expanded CAG repeats. *Nucleic Acids Res.* **39:** 5578-5585.
56. Gagnon, K.; Pendergraff, H.; Deleavey, G.; Swayze, E.; Potier, P.; Randolph, J.; Roesch, E.; Chattopadhyaya, J.; Dahma, M.; Bennett, C.; Montaillier, C.; Lemaitre, M., Corey, DR., (2010). Allele-selective inhibition of mutant huntingtin expression with antisense oligonucleotides targeting the expanded CAG repeat. *Biochemistry* **49:** 10166-78.
57. Hu, J.; Matsui, M.; Gagnon, K. T.; Schwartz, J. C.; Gabillet, S.; Arar, K.; Wu, J.; Bezprozvanny, I.; Corey, D. R., (2009). Allele-specific silencing of mutant huntingtin and ataxin-3 genes by targeting expanded CAG repeats in mRNAs. *Nat. Biotechnol.* **27:** 478-484.
58. Powell, R. M.; Wicks, J.; Holloway, J. W.; Holgate, S. T.; Davies, D. E., (2004). The splicing and fate of ADAM33 transcripts in primary human airways fibroblasts. *Am. J. Respir. Cell Mol. Biol.* **31:** 13-21.
59. Suzuki, Y.; Holmes, J. B.; Cerritelli, S. M.; Sakhuja, K.; Minczuk, M.; Holt, I. J.; Crouch, R. J., (2010). An upstream open reading frame and the context of the two AUG codons affect the abundance of mitochondrial and nuclear RNase H1. *Mol. Cell. Biol.* **30:** 5123-34.

60. Lima, W. F.; Murray, H. M.; Damle, S. S.; Hart, C. E.; Hung, G.; De Hoyos, C. L.; Liang, X. H.; Crooke, S. T., (2016). Viable RNaseH1 knockout mice show RNaseH1 is essential for R loop processing, mitochondrial and liver function. *Nucleic Acids Res* **44:** 5299-312.
61. Hori, S.-I.; Yamamoto, T.; Obika, S., (2015). XRN2 is required for the degradation of target RNAs by RNase H1-dependent antisense oligonucleotides. *Biochem. Biophys. Res. Commun.* **464:** 506-511.
62. Kamola, P. J.; Kitson, J. D.; Turner, G.; Maratou, K.; Eriksson, S.; Panjwani, A.; Warnock, L. C.; Douillard Guilloux, G. A.; Moores, K.; Koppe, E. L.; Wixted, W. E.; Wilson, P. A.; Gooderham, N. J.; Gant, T. W.; Clark, K. L.; Hughes, S. A.; Edbrooke, M. R.; Parry, J. D., (2015). In silico and in vitro evaluation of exonic and intronic off-target effects form a critical element of therapeutic ASO gapmer optimization. *Nucleic Acids Res* **43:** 8638-50.
63. Burel, S. A.; Hart, C. E.; Cauntay, P.; Hsiao, J.; Machemer, T.; Katz, M.; Watt, A.; Bui, H. H.; Younis, H.; Sabripour, M.; Freier, S. M.; Hung, G.; Dan, A.; Prakash, T. P.; Seth, P. P.; Swayze, E. E.; Bennett, C. F.; Crooke, S. T.; Henry, S. P., (2016). Hepatotoxicity of high affinity gapmer antisense oligonucleotides is mediated by RNase H1 dependent promiscuous reduction of very long pre-mRNA transcripts. *Nucleic Acids Res* **44:** 2093-109.
64. Kasuya, T.; Hori, S.; Watanabe, A.; Nakajima, M.; Gahara, Y.; Rokushima, M.; Yanagimoto, T.; Kugimiya, A., (2016). Ribonuclease H1-dependent hepatotoxicity caused by locked nucleic acid-modified gapmer antisense oligonucleotides. *Sci Rep* **6:** 30377.
65. Lennox, K. A.; Behlke, M. A., (2016). Cellular localization of long non-coding RNAs affects silencing by RNAi more than by antisense oligonucleotides. *Nucleic Acids Res* **44:** 863–877.
66. Castanotto, D.; Lin, M.; Kowolik, C.; Wang, L.; Ren, X.-Q.; Soifer, H. S.; Koch, T.; Hansen, B. R.; Oerum, H.; Armstrong, B.; Wang, Z.; Bauer, P.; Rossi, J.; Stein, C. A., (2015). A cytoplasmic pathway for gapmer antisense oligonucleotide-mediated gene silencing in mammalian cells. *Nucleic Acids Res.* **43:** 9350-9361.
67. Gagnon, K. T.; Li, L.; Chu, Y.; Janowski, B. A.; Corey, D. R., (2014). RNAi factors are present and active in human cell nuclei. *Cell Rep* **6:** 211-21.
68. Wang, X.; Li, L.; Xiao, J.; Jin, C.; Huang, K.; Kang, X.; Wu, X.; Lv, F., (2009). Association of ADAM33 gene polymorphisms with COPD in a northeastern Chinese population. *BMC Med. Genet.* **10**.
69. Figarska, S. M.; Vonk, J. M.; van Diemen, C. C.; Postma, D. S.; Boezen, H. M., (2013). ADAM33 Gene Polymorphisms and Mortality. A Prospective Cohort Study. *PLoS One* **8**.
70. Shaffiq, A.; Haitchi, H. M.; Pang, Y. Y.; Alangari, A. A.; Jones, M. G.; Marshall, B. G.; Howarth, P. H.; Davies, D. E.; O'Reilly, K. M. A., (2012). A disintegrin and metalloprotease (ADAM) 33 protein in patients with pulmonary sarcoidosis. *Respirology* **17:** 342-349.
71. Zuker, M., (2003). Mfold web server for nucleic acid folding and hybridization prediction. *Nucleic Acids Res.* **31:** 3406-3415.
72. Koshkin, A. A.; Singh, S. K.; Nielsen, P.; Rajwanshi, V. K.; Kumar, R.; Meldgaard, M.; Olsen, C. E.; Wengel, J., (1998). LNA (Locked Nucleic Acids): Synthesis of the adenine, cytosine, guanine, 5-methylcytosine, thymine and uracil bicyclonucleoside monomers, oligomerisation, and unprecedented nucleic acid recognition. *Tetrahedron* **54:** 3607-3630.
73. Chillemi, R.; Greco, V.; Nicoletti, V. G.; Sciuto, S., (2013). Oligonucleotides Conjugated to Natural Lipids: Synthesis of Phosphatidyl-Anchored Antisense Oligonucleotides. *Bioconj. Chem.* **24:** 648-657.

FIGURE LEGENDS

Figure 1. Types of gene silencing oligonucleotides (left) and chemical modifications (right) used in this study. p=phosphate.

Figure 2. *ADAM33* gene expression can be inhibited by siRNA and ss-siRNA oligonucleotides, but the maximal extent of inhibition is modest. **(A)** Oligonucleotide sequences: 'tt' represents a 3' terminal overhang of two deoxy thymidines, duplex siRNAs are otherwise unmodified RNA; ss-siRNA sequence modifications are '$_s$' (phosphorothioate linkage); red: 2'F-RNA; blue: 2'OMe-RNA; purple: 2'-*O*-MOE-RNA; green: LNA; p (5'-phosphate). For siRNA duplexes, passenger strands are listed on top and guide strands underneath. **(B)** qRT-PCR results from a screen of siRNA duplexes show that very few siRNA sequences were active against this target. **(C)** qRT-PCR results showing gene silencing efficacy of ss-siRNA analogues of the three most potent duplex siRNAs, in comparison with the parent duplexes. **(D)** qRT-PCR results comparing potencies of different chemical modification schemes on ss-siRNA activity. For all figure parts, error bars represent standard deviation of biological replicates. All oligonucleotides were transfected at 50nM into MRC-5 lung fibroblasts using Lipofectamine RNAiMAX. All results are normalized to a scrambled siRNA duplex control.

Figure 3. LNA gapmers are highly potent when transfected with a cationic lipid. **(A)** LNA gapmer sequence modifications are '$_s$' (phosphorothioate linkage); green uppercase: LNA; lower case: DNA. **(B)** qRT-PCR results showing gene silencing by LNA gapmers at 50 nM. All results are normalized to a scrambled siRNA duplex control. Error bars are standard deviation of biological replicates. **(C)** qRT-PCR results showing dose response analysis of **33-O** and **33-R**. Results are normalized to a scrambled LNA gapmer control. Error bars for the dose responses represent standard deviation of technical replicates.

Figure 4. Gymnotically delivered gapmers are potent inhibitors of *ADAM33*. Gene silencing measured by qRT-PCR after gymnotic delivery. Oligonucleotides are delivered to MRC-5 cells at 3µM dose and normalized to a non-treated control (NT). Error bars represent the standard deviation of biological replicates.

Figure 5. Lipid-conjugated LNA gapmers show reduced potency unless the lipid is joined to the ASO via a biocleavable linkage. **(A)** Synthesis and structure of hexadecyloxypropyl LNA conjugates. *Reagents and conditions:* (i) NaH, $CH_3(CH_2)_{15}Br$, cat. KI; (ii) $^{i}Pr_2NP(O(CH_2)_2CN)Cl$, DIPEA, CH_2Cl_2; (iii) standard oligonucleotide synthesis conditions. **(B)** Dynamic light scattering shows that addition of a lipid tail causes self-assembly of ASOs into larger structures (comparing 33-O, red bars, with its biostable conjugate, black bars). **(C)**

qRT-PCR results showing dose response analysis of **A33-N, O**, and **P** and both types of lipid conjugates, after gymnotic delivery to MRC-5 cells at concentrations from 3 to 0.11 μM. Results are normalized to non-treated control sample (NT). Error bars represent standard deviation of biological replicates.

Figure 6. Identification of ASOs that provide highly effective silencing of mouse *Adam33* expression in mouse embryonic fibroblasts. Oligonucleotides were delivered at 50 nM with Lipofectamine RNAiMAX. Error bars represent the standard deviation of biological replicates. Mouse-targeted sequences are shown in Table 1, and were made as fully phosphorothioate (PS) 3-9-3 LNA gapmers (the same chemical architecture as the human sequences). The sequence of LNA-scr2, also a PS 3-9-3 gapmer, is AACacgtctataCGC. **33-O** is the human sequence from figure 3, included as an additional negative control.

TABLE 1 and CAPTION

Name	ASO Sequence
	451 465
33-G	TGATCCGTGTGGTTG
m33-G	TGATCCGTGTGGTTG
	627 641
	2217 2231
33-N	AGGTGTCATGGTTTT
m33-N	AGGCATCTCGGTTTG
	2393 2407
	2575 2589
33-P	TTCATTTTAGGAGCT
m33-P	TAAGCTCAGAGTTCG
	2675 2689
	2577 2591
33-Q	TGTTCATTTTAGGAG
m33-Q	GGTAAGCTCAGAGTT
	2677 2691
	2929 2934
33-R	TCCGTGGAAATTGCA
m33-R	TCTATGACAACAGCT
	2876 2890

Table 1. Design of mouse analogues of lead ASO sequences. Small numbers refer to the base numbering within the target transcripts (in each case human on top, mouse below). Grey highlight in the mouse ASOs represents non-sequence-conserved residues relative to the human ASOs. While P, Q, and R showed only very modest sequence conservation, they showed a greater degree of structural conservation as predicted by T-coffee. RefSeq accession numbers of the sequences used for alignments were as follows: human, NM_025220.3 (3573 nt total length, where the ORF ends at 2569); and mouse, NM_033615.2 (3165 nt total length, where the ORF ends at 2694).